Virchows Arch (1998) 433:75–83

ORIGINAL ARTICLE

A.D. Katsen · B. Vollmar · P. Mestres-Ventura
M.D. Menger

Cell surface and nuclear changes during TNF-α-induced apoptosis in WEHI 164 murine fibrosarcoma cells

A correlative light, scanning, and transmission electron microscopical study

Received: 7 October 1997 / Accepted: 23 March 1998

Abstract Tumour necrosis factor (TNF)-α-induced apoptosis is associated with several nuclear and cell surface alterations, in particular with the condensation of chromatin and the fragmentation of the cell nucleus, formation of blebs on the cell surface and breakdown of the plasma membrane. However, there is little information about the relationship between the cell surface alterations and the nuclear changes during apoptosis. To study this, cultured WEHI cells were exposed to TNF-α over different time periods. The cytological changes were studied using a correlative approach, which allowed observation of the same cell consecutively under light, scanning and transmission electron microscopy. The earliest sign of cell alteration was a reduction of the number of microvilli after 15 min of TNF-α exposure. This reaction was reversible (reappearance of microvilli) and took place during the first hour, in which neither nuclear alterations nor plasma membrane breakdown were observed. The changes in the nucleus began with condensation of chromatin after approximately 1 h of TNF-α-exposure. After 4–5 h the microvilli disappeared again, particularly in areas where the formation of blebs (blebbing) was observed. Strikingly, cell surface alterations (bleb formation) were detected only in those cells that presented with condensed chromatin, and not in cells with a normal chromatin pattern, proving at least a close correlation between nuclear and cell surface changes during the process of apoptosis.

Key words Apoptosis · Cell surface · Cell nucleus · Blebs · TNF-α · Electron microscopy

A.D. Katsen · B. Vollmar · M.D. Menger (✉)
Institute for Clinical and Experimental Surgery,
University of Saarland, D-66421 Homburg/Saar, Germany
e-mail: exmdme@ med-rz.uni-sb.de,
Tel.: (+49)-6841-16-6550/1, Fax: (+49)-6841-16-6553

A.D. Katsen · P. Mestres-Ventura
Institute of Anatomy, University of Saarland,
Homburg/Saar, Germany

Introduction

Tumour necrosis factor (TNF)-α is a pleiotrophic cytokine capable of inducing biological reactions, such as inflammation, septic shock, cachexia, and cell proliferation [2, 28]. In vitro TNF-α is cytotoxic for transformed and non-transformed cell lines, inducing both forms of cell death, apoptosis and necrosis [4, 9, 14, 16]. Apoptosis is characterized by nuclear changes, such as chromatin condensation and fragmentation of the nucleus, loss of cell volume, and blebbing with preservation of plasma membrane integrity [32]. In contrast, necrosis is associated with organelle swelling, membrane breakdown, and cell disintegration [32].

Cellular alterations associated with TNF-α-induced apoptosis and necrosis may appear at different time points, having a strongly individual character for each single cell. In order to clarify a possible relationship/dependency between early changes at the cell surface and in the cell nucleus, it is important to obtain precise information on the course of the distinct nuclear and plasma membrane alterations induced by TNF-α. For this purpose, a correlative technique combining light, scanning and transmission electron microscopy was used. Condensation of chromatin and breakdown of the plasma membrane were detected using DNA fluorochromes and light microscopy, whilst the corresponding structural modifications were determined by electron microscopy. All these observations were performed in the same cell by means of a locally devised method of producing landmarks in the substrate allowing re-localization of a cell at the different stages of microscopical investigation.

Materials and Methods

Highly TNF-α-sensitive methylcholanthrene-induced mouse fibrosarcoma cells [WEHI 164/clone 13 (WEHI)] were cultured in a concentration of 1×10^5 cells/ml on circular glass slides in RPMI 1640 medium supplemented with 10% fetal serum, 0.1 mM glutamine and gentamicin (30 μg/ml). The glass slides were shadowed with indium oxide [22], marked with a diamond indentor [25] and

coated with 20 mg/ml poly-L-lysin (Sigma, St. Louis, Mo.). After 24 h of cell culture and change of medium, 200 U/ml recombinant TNF-α (Boehringer, Mannheim, Germany) was added to the cells.

After different periods of TNF-α-exposure (15 min, 1, 2, 4, 5, and 6 h) the cells were stained intravitally with H 33342 (Sigma; 2.0 μg/ml in Hepes buffer) for 20 min and with ethidium bromide (EB, Sigma; 5.0 μg/ml in Hepes buffer) for 10 min. Controls without TNF-α exposure were analysed at identical time points. For microscopical examination, the specimens were kept in Hepes buffer solution. Only cells attached to the substrate were included in our analysis. Cells located within the area marked with the diamond were photographed under phase contrast and fluorescence microscopy (MX60F Olympus). Under ultraviolet (UV) epi-illumination (excitation wavelength: 330–380 nm; emission wavelength: >430 nm), H33342 stained the nuclei of cells with intact cell membrane (blue), whereas EB stained only the nuclei of cells with damaged plasma membrane [red with the green emission filter (530–560 nm/>580 nm) or pink with the UV filter]. In some experiments the distribution of F-actin after 5 h of TNF-α exposure was determined as follows. Cells were first stained with H33342, washed in Hepes, fixed in buffered formaldehyde (2%, pH 7.4) and then labelled with RITC-phalloidin (rhodamin-isothiocyanate-phalloidin, 5 μg/ml, Molecular Probes, Eugene, Ore.) [17].

For scanning electron microscopy (SEM), the cells were washed in Hepes and fixed overnight in 2% glutaraldehyde buffered with 0.12 M sodium cacodylate (pH 7.4). The postfixation was performed in three steps using 1% osmium tetroxide, 1% tannic acid and 1% uranyl acetate, a schedule especially developed for SEM [13]. After dehydration in ethanol, specimens were critical-point-dried and sputtered with gold (~5 nm thick). Cells previously identified in light microscopy were relocalized using the diamond marks as landmarks [13]. The specimens were examined with a CamScan S2 (Cambridge, UK) scanning electron microscope at 20 kV.

After SEM examination, specimens were prepared for transmission electron microscopy (TEM) by embedding in Araldite 502 and removing from the substrate after polymerization [13]. Again, the diamond replica served to relocalize the cells that were to be cut with the ultramicrotome. The ultrathin sections were stained with lead citrate and examined in a Zeiss EM 10 CR transmission electron microscope at 60 kV.

In this investigation only cells attached to the substrate were considered for statistical analysis. The numbers of cells presenting with changes in the nucleus or on the surface are given as percentages of all cells analysed (see Table 1). The apoptotic and necrotic alterations were analysed in relation to the time of exposure to TNF-α and compared with controls not exposed to TNF-α, using the χ^2-test including the Yates correction.

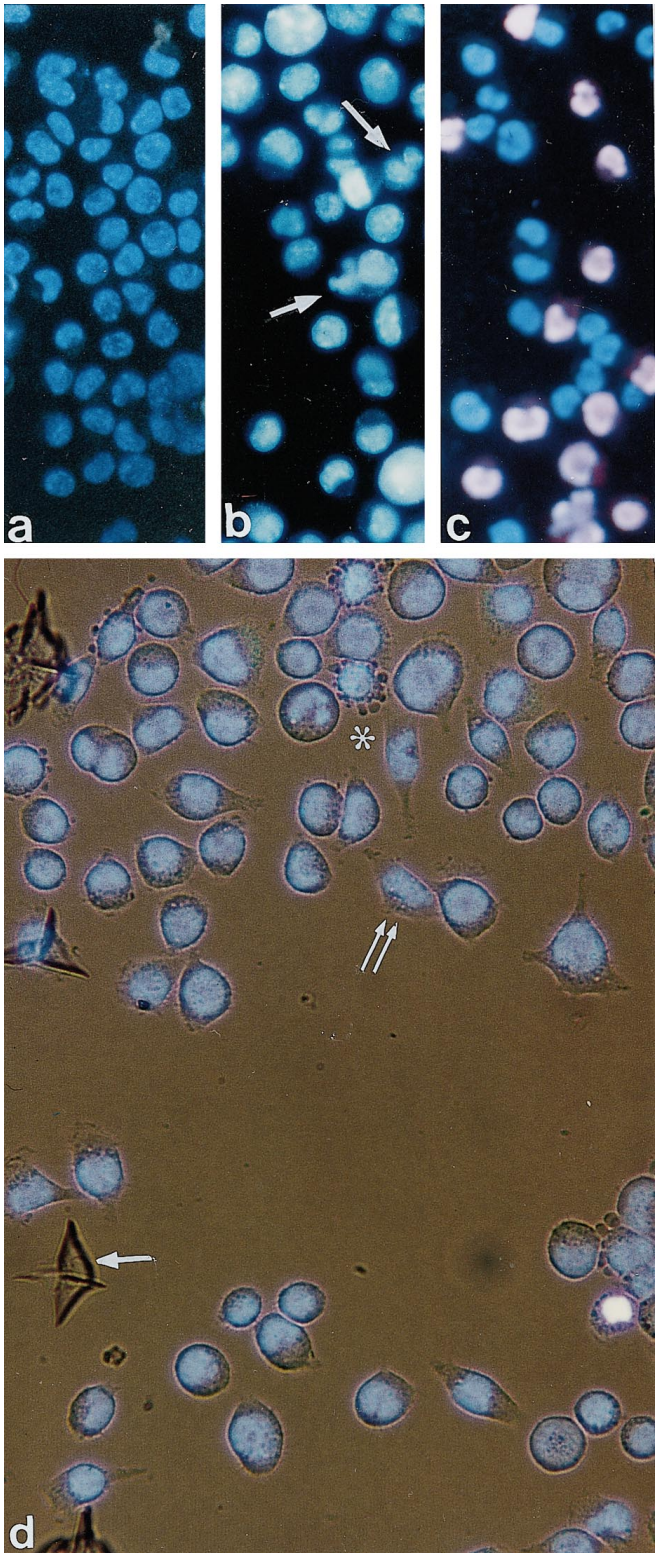

Results

In control preparations the WEHI cells seen with the phase contrast microscope displayed a polymorphic shape, varying from polygonal to round. All cells were attached to the substrate, including those with a spherical shape. Under these conditions blebbing was not observed. The majority of WEHI cells (~99%) showed a nucleus well stained with H 33342 and displaying a nor-

Fig. 1 **a–c** Fluorescence microscopy and **d** phase contrast combined with fluorescence microscopy of WEHI cells. Nuclei of intact cells show blue fluorescence staining, nuclei of damaged cells present with a fluorescence in pink (*EB*). **a** Control conditions. ×400 **b** After 5 h of TNF-α exposure individual cells present with condensed chromatin. Some cells show nuclear fragmentation (*arrows*). ×400 **c** After 6 h of TNF-α exposure the number of EB-stained cells is markedly increased compared with that of the previous stages. Because of detachment from the substrate these cells often appear out of focus. ×400 **d** After 5 h of TNF-α exposure cells with condensed chromatin (*asterisk*) and cells with a normal chromatin pattern (*double arrows*) are a common finding. Blebs are only observed in those cells with condensed chromatin pattern (*asterisk*). *Arrow* diamond indentation. ×480

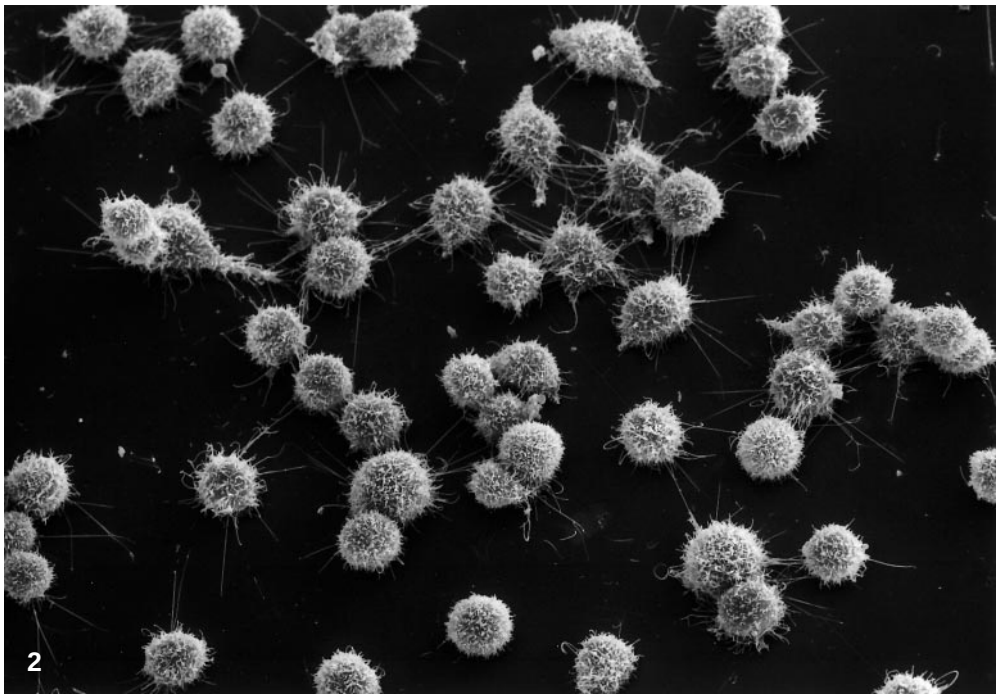

Fig. 2 Scanning electron microscopy of WEHI cells under control conditions. The cell surface is densely covered with microvilli. ×720

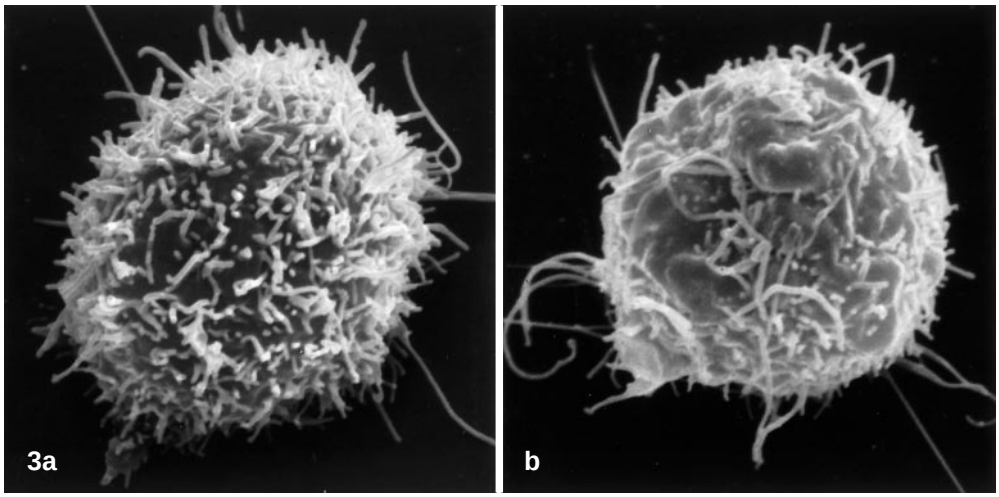

Fig. 3 Scanning electron microscopy of a WEHI cell **a** under control conditions and **b** after 15 min TNF-α exposure. Note in (**b**) the reduction of the number of microvilli. ×4800

Table 1 Apoptosis-induced chromatin condensation (CC) and fragmentation (CF) as well as plasma membrane damage (EB-positive staining) and cell surface bleb formation (BF) in WEHI 164/clone 13 cells after TNF-α-exposure.

Time after	number of cells (n)		CC (%)		CF (%)		EB+ (%)		BF (%)	
TNF-α	C	TNF	C	TNF	C	TNF	C	TNF	C	TNF
Baseline	565		0		0		0.9		0	
1 hour	244	238	0.8	5.0*	0.8	0.8	0.8	2.1	0	0
2 hours	361	353	1.7	5.7*	0.3	0.8	0.6	0.3	0	0.6
4 hours	315	275	2.9	32.4*	0.3	3.6*	1.0	5.5*	0	10.9*
5 hours	287	240	1.7	80.8*	0.3	5.0*	1.0	5.0*	0	12.1*
6 hours	110	81	2.7	32.1*	0	3.7*	0.9	49.4*	0	0

C = controls without TNF-α-exposure, TNF = cells exposed to TNF-α; values are given in percent of all cells analyzed. χ^2-test, including Yates correction; *P <0.05 vs baseline and corresponding controls.

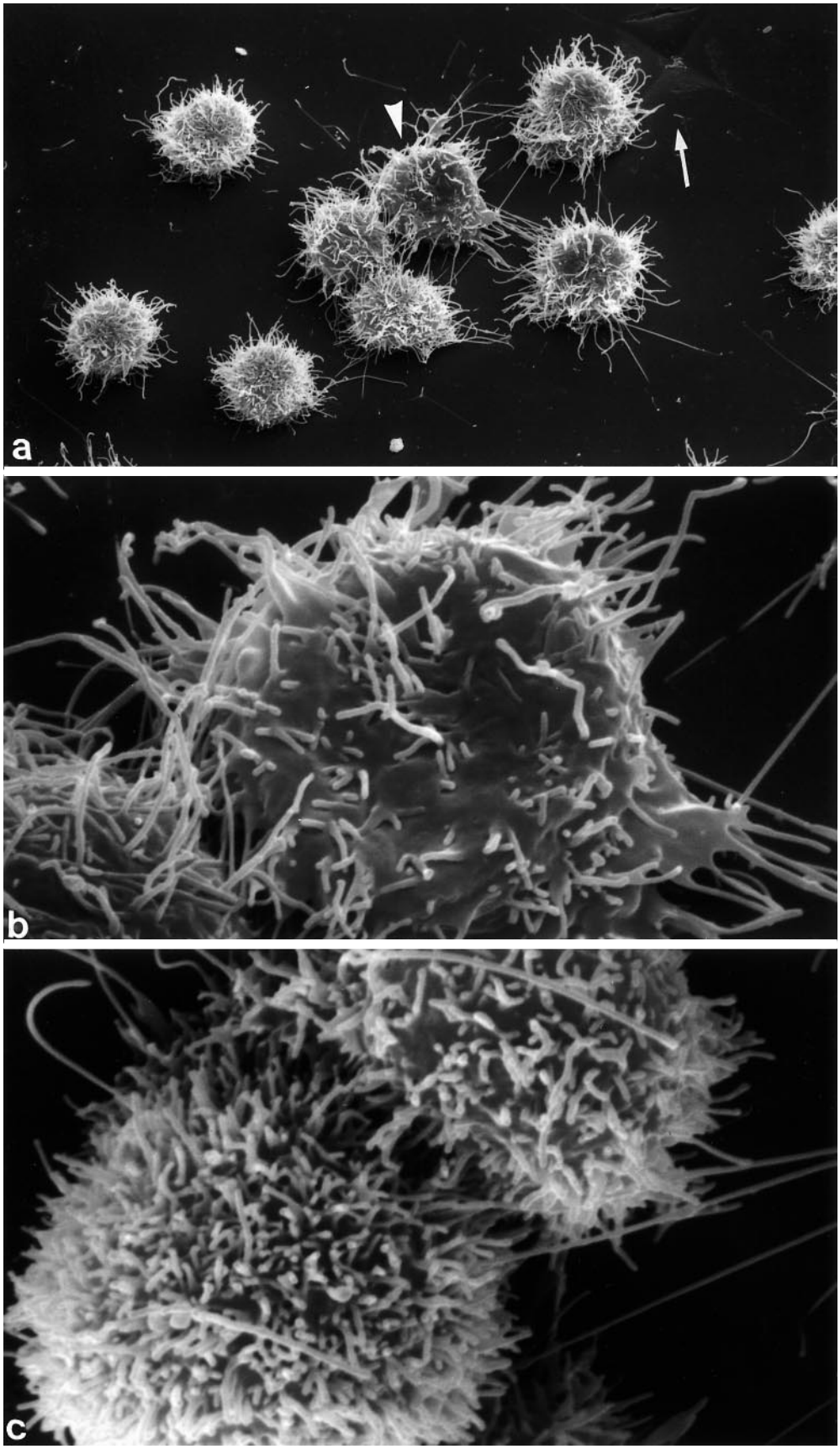

Fig. 4 Scanning electron microscopy of WEHI cells **a, b** after 4 h of TNF-α exposure and **c** under control conditions. **a** Overview. *Arrow* diamond indentation. ×1200 **b** Detail of the cell labelled with *arrowhead* in **a**. Note that only few microvilli are present at the 'top' of the adherent cell (see also Fig. 6b); for comparison see cell surface distribution of microvilli under control conditions (**c**). ×6660 **c** Detail of the surface of two WEHI cells under control conditions. ×6660

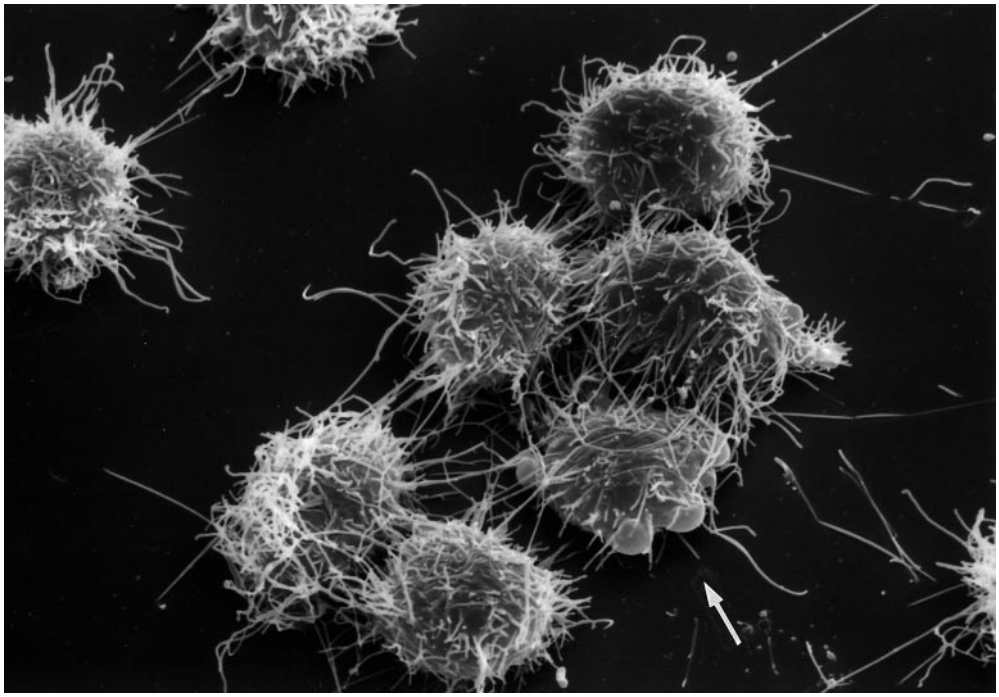

Fig. 5 Scanning electron microscopy of WEHI cells after 4 h of TNF-α exposure. Some cells (*arrow*) show both loss of microvilli and formation of blebs. ×2000

mal chromatin pattern (Fig. 1a). Cells in mitosis (0.7–2.9%) presented a condensed chromatin pattern with intense fluorescence, which made them easily distinguishable from non-mitotic cells. Only a few cells showed nuclear staining with EB under normal conditions (~1%, see Table 1).

After TNF-α exposure the percentage of cells with condensed chromatin increased progressively, with values of 5.0% after 1 h rising to 80.8% after 5 h of cytokine exposure (Table 1, Fig. 1b). Cell counts revealed that the mitotic fraction remained unchanged after TNF-α exposure. Nuclear fragmentation was observed first in those cells in which chromatin was previously condensed. The percentage of cells showing chromatin fragmentation increased during the TNF-α exposure (Table 1). During this time the percentage of EB-stained cells also increased slightly, with values of ~5% after 5 h of TNF-α exposure. Strikingly, these cells and their nuclei were normal in size and volume. After an TNF-α exposure period of 6 h or longer, the fraction of cells with breakdown of the plasma membrane, as visualized by EB staining, increased dramatically, with values up to 50% (Table 1, Fig. 1c). However, after these periods of cytokine exposure the cells became detached, making it difficult to perform differential quantitation with the current technical approach. Thus, aspects involving long cytokine exposure times, such as apoptotic body formation, could not be included in the present investigation.

Analysis of bleb formation revealed the first signs after 4 h of TNF-α exposure (Table 1). At this stage approximately 10% of the cells analysed showed blebs. Most strikingly, blebbing was observed only in cells with a condensed chromatin pattern. Neither cells with a normal chromatin pattern nor those with EB-positive nuclei showed bleb formation on their surface (Fig. 1d). The proportion of cells presenting with blebs was still significantly increased after 5 h of TNF-α exposure (Table 1), but was found to be zero after 6 h, which was probably due to detachment of these cells from the substrate.

Staining with RITC-phalloidin revealed that after 5 h of TNF-α exposure F-actin was abundant in the cell body, but was lacking in the blebs (not shown).

On SEM, control WEHI cells displayed a variable grade of spreading, which is in agreement with the polymorphism seen by LM. However, density of microvilli was rather high and not dependent on the grade of cell spreading (Fig. 2). Initial cell surface changes were observed after as little as 15 min TNF-α exposure. At this time the number of microvilli appeared to be strikingly reduced when compared with controls (Fig. 3). However, this was a reversible modification of the cell surface, since at 1 h the microvilli reappeared with a density similar to that observed in controls (Fig. 3). A distinct loss of microvilli, particularly pronounced at the ‘top’ of the adherent cells, was observed again after 4 h of TNF-α exposure (Fig. 4). These changes were detected before the first blebs originated at the cell surface (Figs. 5, 6b). One hour later (after 5 h of cytokine exposure) the blebs had increased in number and size (Fig. 6c). The correlative LM/SEM examination confirmed the assumption that only cells with condensed chromatin presented evident blebbing (Figs. 6, 7). In some cases blebs were distributed over the whole cell surface, and this was regularly accompanied by a tremendously decreased density of microvilli (Figs. 6c, 7b).

Using the correlative method described above, single cells treated for 5 h with TNF-α were examined first

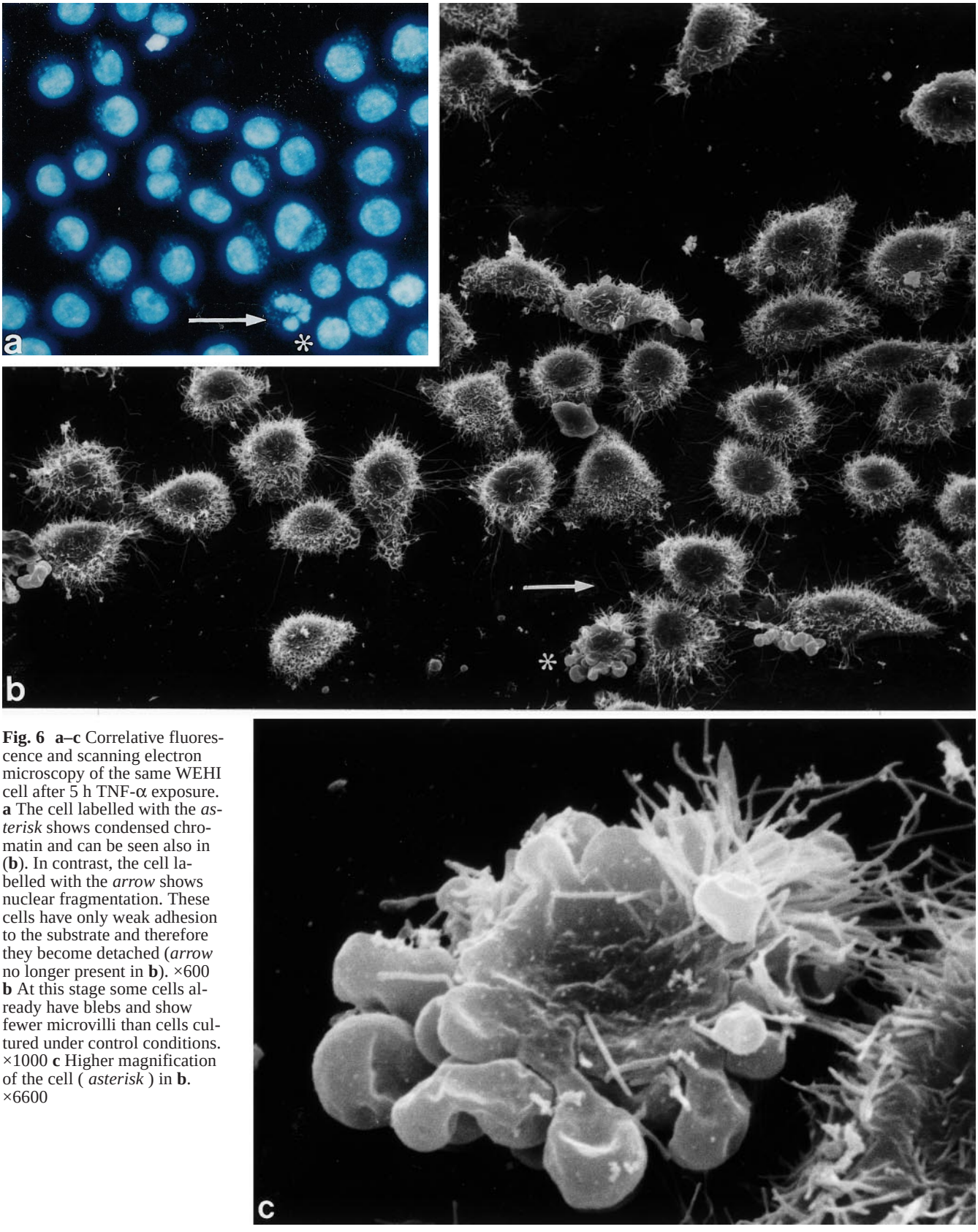

Fig. 6 **a–c** Correlative fluorescence and scanning electron microscopy of the same WEHI cell after 5 h TNF-α exposure. **a** The cell labelled with the *asterisk* shows condensed chromatin and can be seen also in (**b**). In contrast, the cell labelled with the *arrow* shows nuclear fragmentation. These cells have only weak adhesion to the substrate and therefore they become detached (*arrow* no longer present in **b**). ×600 **b** At this stage some cells already have blebs and show fewer microvilli than cells cultured under control conditions. ×1000 **c** Higher magnification of the cell (*asterisk*) in **b**. ×6600

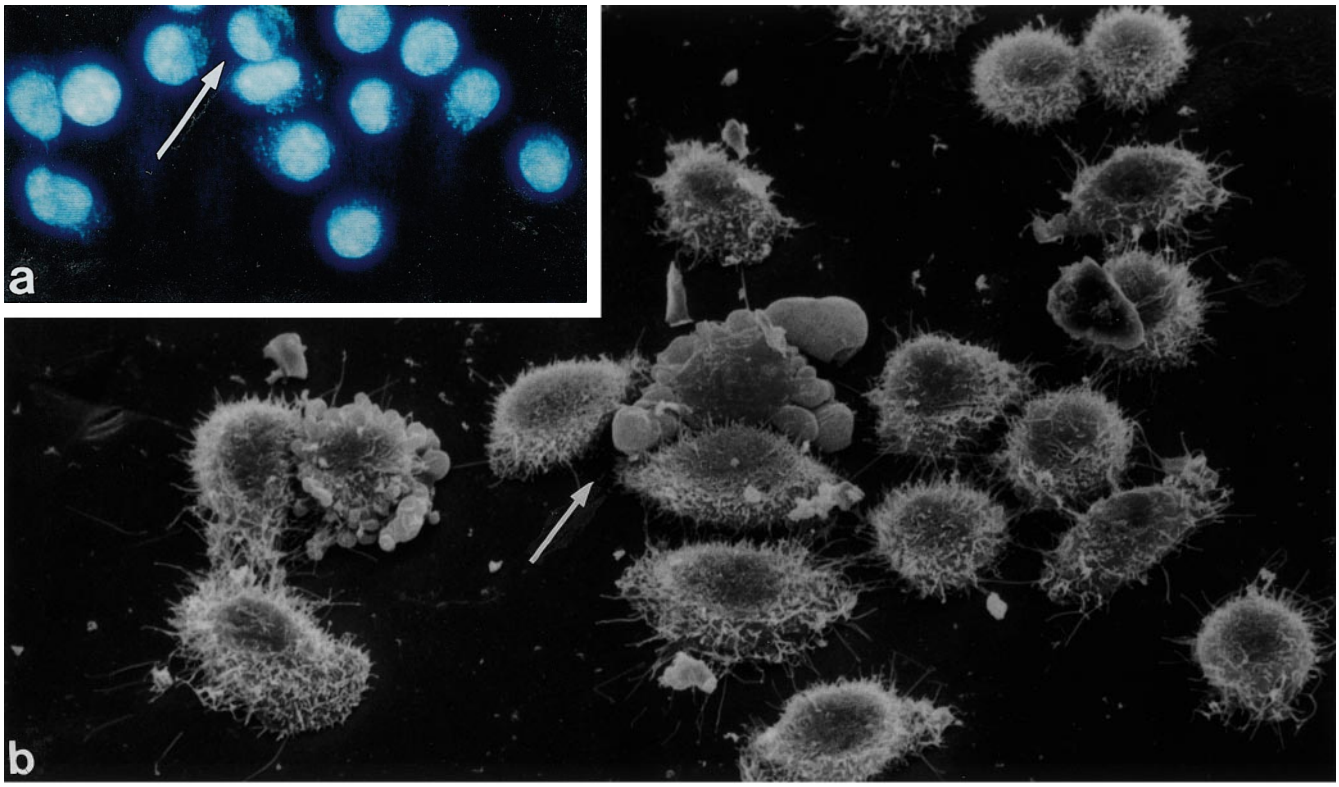

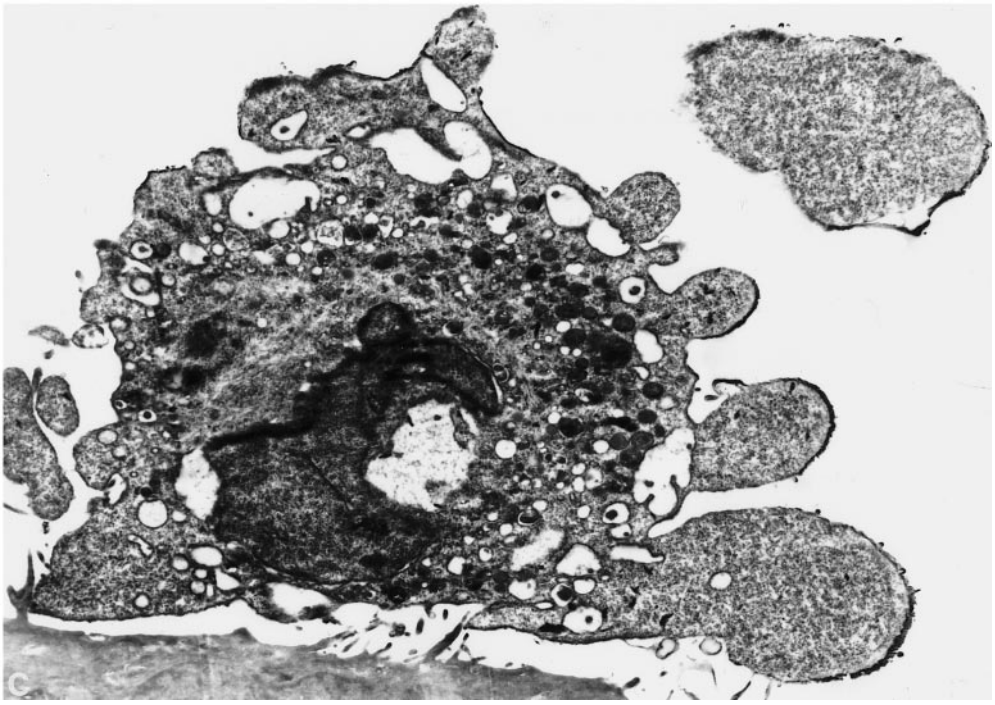

Fig. 7 **a** Correlative fluorescence microscopy, **b** scanning and **c** transmission electron microscopy of the same WEHI cell after 5 h of TNF-α exposure. The cell investigated is labelled with a *white arrow* in **a** and **b**, and a ultrathin section of it is illustrated in **c**. **a** The cell shows chromatin condensation. ×600 **b** Blebs can be seen and microvilli are almost disappeared. ×1200 **c** The nucleus is altered in shape, and the space of the nuclear membrane in some places appears enlarged. The perinuclear area of the cytoplasm is occupied by microfilaments, displacing the organelles towards the periphery. The vacuoles located at the outer area of the cytoplasm may correspond to expanded parts of rough endoplasmic reticulum. The blebs do not contain organelles. ×7200

with LM, subsequently with SEM and finally with TEM (Fig. 7). Cells with blebs in ultrathin sections displayed nuclei in advanced stages of chromatin condensation and sometimes already in the early phase of fragmentation. Moreover, the space of the nuclear membrane and the cisternae of the endoplasmic reticulum appeared distended (Fig. 7c). Bundles of microfilaments occupied a rather wide field between the nuclear membrane and the cisternae of the endoplasmic reticulum (Fig. 7c). In all cells examined, blebs were devoid of organelles, containing only a fine granulated matrix and few small vesicles. Specific arrangements of the cytoskeleton in relation to the blebs and their necks was not observed (Fig. 7c)

Discussion

WEHI cells correspond to a line derived from fibrosarcoma cells of Balb/c origin induced by methylcholanthrene [6]. Because these cells are very sensitive to TNF-α exposure, which produces cell death [5, 6], they are frequently used in studies dealing with the toxicity of TNF-α [31]. The relevant literature offers differing opinions as to the ability of TNF-α to induce cell death in vitro. Whereas some authors consider that it causes both apoptosis and necrosis, for instance in L-929 cells or WEHI cells [7, 16], other groups who are also working with WEHI cells have presented evidence that only apoptosis can be induced [27]. Our observations do not support the latter interpretation. After 5 h exposure to TNF-α we clearly detected a small cell population of EB-positive cells. The fact that the size and the volume of these cells and their nuclei were normal indicates that primary damage of the cell membrane, which is characteristic of necrosis, has occurred, rather than the secondary membrane damage seen in apoptotic cells. The dramatic increase in the number of EB-positive cells after 6 h of TNF-α exposure suggests that necrosis is a delayed reaction compared with apoptosis. The detachment of these cells without re-adherence over a period of 24 h (data not shown) indicates the irreversibility of the alterations.

Our study, however, was focused on the cellular alterations occurring during the first 5–6 h of TNF-α exposure. The cytological alterations observed during this period can be divided into three phases. The first phase corresponds to the first hour of TNF-α exposure, with changes taking place solely at the cell surface (disappearance and reappearance of microvilli). The second phase extends to the 4th and 5th hours and is characterized first by changes in the nucleus (condensation and fragmentation of chromatin) and secondly, again, by alterations of the cell surface (irreversible disappearance of microvilli and bleb formation). The study of the third phase was limited in our experiments to the interval between the 5th and 6th hours of TNF-α exposure, demonstrating the breakdown of the cell membrane as the most representative phenomenon.

The first signs of alteration induced by TNF-α were the reduction in the number of microvilli and their reappearance during the first hour of exposure to TNF-α. The fact that this response was reversible is worthy of note. Considering its similarity to responses against ionizing radiations and low temperature, it may be interpreted as a reaction of cell stress [1, 11]. However, these early changes to the cell surface may be related to the interactions between the ligand TNF-α and its receptors, TNF-R1 and TNF-R2 [19, 30]. In vitro studies with several cell lines have shown that unoccupied insulin receptors are localized at the membrane of microvilli, whereas the occupied ones appear to be confined to the non-villous membrane [3]. The receptors of the non-villous domains of the membrane bind to the corresponding ligands and become internalized before they can be recycled back to the cell surface [3]. A similar mechanism could apply to our case with TNF-α and WEHI-cells. This rationale, however, does not explain the disappearance of microvilli observed after 4 h of TNF-α exposure. This change is different from that observed during the first hour of cytokine exposure: specifically, it was restricted to a rather small area of the cell surface and it preceded the formation of blebs.

The metabolic situation of cells with evident signs of apoptosis (chromatin condensation) is quite different, and it is probable that the cytoskeleton is involved in the processes of cell surface changes. It is generally accepted that actin is responsible for the dynamics of microvilli and cell membrane [8, 17]. Actin can polymerize and depolymerize very fast in all parts of the cell [24], but although changes in the distribution and reorganization of F-actin can explain the disappearance of microvilli, its role in the formation of apoptotic blebs is not clear. In agreement with previous studies, the apoptotic blebs do not contain F-actin [15, 17, 26]; only at the base of blebs appearing in apoptotic cells were microfilaments observed [15]. The knowledge that blebs of mitotic cells contain F-actin not only at the neck but also in the bleb itself [15] excludes the possibility that the bleb formation observed in our experiments was due to mitosis.

The mechanism of condensation of the chromatin during apoptosis is different from that occurring in mitosis [21]. The chromatin condensation related to mitosis is mediated by the activation of $p34^{cdc2}$ kinase and accompanied by a reversible solubilization of lamin [10]. At the onset of apoptosis a small amount of lamin also solubilizes, but nevertheless, irreversible lamin degradation accompanies apoptotic chromatin condensation [20, 21]. Chromatin condensation during apoptosis is mediated by rapid proteolysis of nuclear cytoskeletal proteins without mediation of $p34^{cdc2}$ kinase [20, 21]. Lamin may be related to the shape of the nucleus, so that deformations of the nuclear membrane and changes in shape of the cell nucleus might be related to lamin degradations.

Cell detachment has been described in both mitotic and apoptotic cells; however, the former retain their ability to adhere [29]. Detachment means that changes or modifications take place not only in the cytoskeleton but also at the cell membrane, with a diminution of the adhesive forces and adhesive properties of the cell to the substrate. A disruption of the actin filaments seems to be involved in cell detachment during the advanced stages of cell death [23]. In our experiments rearrangement of microfilaments was observed, but not their disruption. Probably disruption of microfilaments is a modification that comes about in the advanced stages of apoptosis rather than in the early periods included in the scope of our study.

During apoptosis induced by TNF-α two types of blebs can be distinguished. In the early phases (the interval considered in our experiments) blebs do not contain any organelles, but they merely show a fine granulated matrix without filamentous structures and with few vesicles. This is a distinct type of bleb, which has been repeatedly described in other cell lines undergoing apopto-

sis [15, 18]. The blebs developed by the WEHI cells in our experiments correspond to this type. Another type of bleb, the so-called apoptotic bodies, appears in advanced stages of the apoptotic process. In this second type DNA is commonly found (nuclear material that can be stained with DNA fluorochromes – see Materials and methods [12]). Preliminary studies suggest that these second type of blebs can be cut off and may represent a mechanism of release of nuclear fragments into the medium. This type of bleb, however, could not be analysed in our experiments, probably because cellular detachment after prolonged periods of TNF-α exposure made it impossible to get hold of those individual remnant bodies.

In conclusion, in agreement with others [21] our study demonstrates that the first changes characteristic of apoptosis appear in the nucleus. The correlative investigation of a cell with light and electron microscopy, however, adds new aspects on the behaviour of the cell surface during the early stages of apoptosis and allows a more precise description of the course of this phenomenon. According to our observations, only cells in advanced stages of chromatin condensation develop blebs, proving at least a close correlation between nuclear and cell surface changes during the process of apoptosis.

Acknowledgements This study was supported by grants from the Wilhelm Sander Foundation (93.019.01), the Deutsche Forschungsgemeinschaft (Vo 450/5-1), and the EU (BMH 4-CT95-0875). The authors thank Mrs G. Kiefer and Mr. N. Pütz for excellent technical assistance. B.V. is supported by a Heisenberg-Stipendium of the Deutsche Forschungsgemeinschaft.

References

1. Andrushkevich VV, Serebriakov NG, Kalendo GS (1987) Changes in the surface micro-contour of cells after exposure to ionizing radiation. Dokl. Akad. Nauk SSSR 293:976–978
2. Beutler B, Cerami A (1989) The biology of cachectin/TNF – a primary mediator of the host response. Annu Rev Immunol 7:625–655
3. Carpentier JL (1994) Insulin receptor internalization: molecular mechanisms and physiopathological implications. Diabetologia 37:S117–124
4. Carswell EA, Old LJ, Kassel RL, Green S, Fiore N, Williamson BD (1975) An endotoxin-induced serum factor that causes necrosis of tumors. Proc Natl Acad Sci USA 73:3666–3670
5. Eskandari MK, Nguyen DT, Kunkel SL, Remick DG (1990) WEHI 164 subclone 13 assay for TNF: sensitivity, specificity, and reliability. Immunol Invest 19:69–79
6. Espevik T, Nissen-Meyer J (1986) A highly sensitive cell line, WEHI 164 clone 13, for measuring cytotoxic factor/tumor necrosis factor from human monocytes. J Immunol Methods 95:99–105
7. Fady C, Gardner A, Jacoby F, Briskin K, Tu Y, Schmid I, Lichtenstein A (1995) Atypical apoptotic cell death induced in L 929 targets by exposure to tumor necrosis factor. J Interferon Cytokine Res 15:71–80
8. Follett EAC, Goldman RD (1970) The occurence of microvilli during spreading and growth of BHK/C13 fibroblasts. Exp Cell Res 59:124–136
9. Fransen L, van der Heyden J, Ruysschaert R, Fiers W (1986) Recombinant tumor necrosis factor: Its effect and its synergism with interferon-γ on a variety of normal and transformed human cell lines. Eur J Cancer Clin Oncol 22:419–426
10. Gerace L, Blobel G (1980) The nucelar envelope lamina is reversibly depolymerized during mitosis. Cell 19:277–287
11. Katsen AD, Rickberg AB (1991) A method of phase-contrast, fluorescence and scanning electron microscopy of one and the same cultured cells undergoing cryogenic action. Tsitologiia 33:76–81
12. Katsen A, Menger MD, Mestres P (1996) Changes of the cell surface of L-929 cells induced by TNF-α. Light and scanning electron microscopic correlative study. Beitr Elektronenmikoskop Direktabb Anal Oberfl 29:193–200
13. Katsen AD, Tregubova NA, Andrushkevich VV, Rovensky YA (1992) Identification and study of the same cell in monolayer culture by different methods of light microscopy, scanning and transmission electron microscopy. Application for cryodamaged cells examination. Scanning 14:225–230
14. Kyprianou N, Alexander RB, Isaacs JT (1991) Activation of programmed cell death by recombinant human tumor necrosis factor plus topoisomerase II-targeted drugs in L 929 tumor cells. J Natl Cancer Inst 83:346–350
15. Laster SM, Mackenzie JM Jr (1996) Bleb formation and F-actin distribution during mitosis and tumor necrosis factor-induced apoptosis. Microsc Res Tech 34:272–280
16. Laster SM, Wood JG, Gooding LR (1988) Tumor necrosis factor can induce both apoptotic and necrotic forms of cell lysis. J Immunol 141:2629–2634
17. Leopardi E, Friend DS, Rosenau W (1984) Target cell lysis: ultrastructural and cytoskeletal alterations. J Immunol 133:3429–3436
18. Malorni W, Iosi F, Mirabelli F, Bellomo G (1991) Cytoskeleton as a target in menadione-L induced oxidative stress in cultured mammalian cells: alterations underlying surface bleb formation. Chem Biol Interact 80:217–236
19. Nagata S (1997) Apoptosis by death factor. Cell 88:355–365
20. Neamati N, Fernandez A, Wright S, Kiefer J, McConkey DJ (1995) Degradation of lamin B_1 precedes oligonucleosomal DNA fragmentation in apoptotic thymocytes and isolated thymocyte nuclei. J Immunol 154:3788–3795
21. Oberhammer FA, Hochegger K, Fröschl G, Tiefenbacher R, Pavelka M (1994) Chromatin condensation during apoptosis is accompanied by degradation of lamin A+B, without enhanced activation of cdc2 kinase. J Cell Biol 126:827–837
22. Ogura K, Kuscheck D (1980) Direct observation of light microscopy specimen with electron microscopy. Eur J Cell Biol 22:610
23. Palladini G, Finardi G, Bellomo G (1996) Disruption of actin microfilament organization by cholesterol oxides in 73/73 endothelial cells. Exp Cell Res 223:72–82
24. Papakonstanti EA, Emmanouel DS, Gravanis A. Stournaras C (1996) Na^+/Pi co-transport alters rapidly cytoskeletal protein polymerization dynamics in opossum kidney cells. Biochem J 315:241–247
25. Rickberg AB, Katsen AD, Chumak SM (1984) Precise method for identification and study of individual cells by light and scanning electron microscopy. Scanning 6:183–186
26. Scanlon M, Laster SM, Wood JG, Gooding LR (1989) Cytolysis by tumor necrosis factor is preceded by a rapid and specific dissolution of microfilaments. Proc Natl Acad Sci USA 86: 182–186
27. Shih SC, Stutman O (1996) Cell cycle-dependent tumor necrosis factor apoptosis. Cancer Res 56:1591–1598
28. Tracey KJ, Cerami A (1993) Tumor necrosis factor, other cytokines and disease. Annu Rev Cell Biol 9:317–343
29. Traganos F, Kimmel M, Bueti C, Darzynkiewicz Z (1987) Effects of inhibition of RNA or protein synthesis on CHO cell cycle progression. J Cell Physiol 133:277–287
30. Tsujimoto M, Yip YK, Vilček J (1985) Tumor necrosis factor: Specific binding and internalization in sensitive and resistant cells. Proc Natl Acad Sci USA 82:7626–7630
31. Wanner G, Ertel W, Möller P, Hüfer Y, Leiderer R, Menger MD, Messmer K (1996) Liver ischemia and reperfusion induces systemic inflammatory response through Kupffer cell activation. Shock 5:34–40
32. Wyllie AH, Kerr JFR, Currie AR (1980) Cell death: the significance of apoptosis. Int Rev Cytol 68:251–306